Steady-State Kinetic Mechanism of Recombinant Avocado ACC Oxidase: Initial Velocity and Inhibitor Studies†

Norbert M. W. Brunhuber,‡,§ Jessica L. Mort,‡ Rolf E. Christoffersen,§ and Norbert O. Reich*,‡

Department of Chemistry and Biochemistry and Department of Molecular, Cellular, and Developmental Biology, University of California, Santa Barbara, Santa Barbara, California 93106

Received January 4, 2000; Revised Manuscript Received May 19, 2000

ABSTRACT: The gaseous plant hormone ethylene modulates a wide range of biological processes, including fruit ripening. It is synthesized by the ascorbate-dependent oxidation of 1-aminocyclopropyl-1-carboxylate (ACC), a reaction catalyzed by ACC oxidase. Recombinant avocado (*Persea americana*) ACC oxidase was expressed in *Escherichia coli* and purified in milligram quantities, resulting in high levels of ACC oxidase protein and enzyme activity. An optimized assay for the purified enzyme was developed that takes into account the inherent complexities of the assay system. Fe(II) and ascorbic acid form a binary complex that is not the true substrate for the reaction and enhances the degree of ascorbic acid substrate inhibition. The K_d value for Fe(II) (40 nM, free species) and the K_m's for ascorbic acid (2.1 mM), ACC (62 μM), and O_2 (4 μM) were determined. Fe(II) and ACC exhibit substrate inhibition, and a second metal binding site is suggested. Initial velocity measurements and inhibitor studies were used to resolve the kinetic mechanism through the final substrate binding step. Fe(II) binding is followed by either ascorbate or ACC binding, with ascorbate being preferred. This is followed by the ordered addition of molecular oxygen and the last substrate, leading to the formation of the catalytically competent complex. Both Fe(II) and O_2 are in thermodynamic equilibrium with their enzyme forms. The binding of a second molecule of ascorbic acid or ACC leads to significant substrate inhibition. ACC and ascorbate analogues were used to confirm the kinetic mechanism and to identify important determinants of substrate binding.

Ethylene is a colorless gas synthesized by all plants and involved in many plant processes including rooting, fruit ripening, abscission, and senescence (*1*). The ethylene biosynthetic pathway includes the formation of ACC[1] from *S*-adenosylmethionine followed by oxidative breakdown of ACC to ethylene, CO_2, and HCN. These final two steps in the pathway are catalyzed by ACC synthase and ACC oxidase, respectively (*2*, *3*). ACC oxidase activity was initially described in vivo by Adams and Yang (*4*). The first in vitro observation of ACC oxidase was from melon fruit (*5*), followed by a number of other fruit tissues including apple (*6*−*7*) and avocado (*8*).

ACC oxidase (1-aminocyclopropyl-1-carboxylate, ascorbate:oxygen, decyclizing with no oxygen incorporation; EC 1.X.X.X) is a mononuclear nonheme iron enzyme which binds Fe(II), O_2, AA, and ACC. It is a member of a family of nonheme iron- and ascorbate-dependent oxidases (*9*). ACC oxidase catalyzes two carbon−carbon bond cleavages in an ascorbate-dependent manner to form ethylene, cyanoformate, and dehydroascorbate (Scheme 1; *5*, *8*, *10*). Cyanoformate is known to decompose into cyanide and CO_2 (*11*, *12*). However, it is not definitively known whether this happens in solution or at the active site. Since oxygen is not found in any products, it is likely to undergo a concomitant four-electron reduction to two water molecules. The molecular fate of each carbon within ACC is known (Scheme 1; *11*). High levels of CO_2 were shown to increase the enzyme's V_{max} and K_m^{ACC} by an unknown mechanism (*10*, *13*, *14*).

Other members of this enzyme family are distinguished by their cosubstrate requirement. Mechanistically well studied enzymes which require α-ketoglutarate include prolyl hydroxylase (*15*), lysyl hydroxylase (*16*), γ-butyrobetaine hydroxylase (*17*), and thymine 7-hydroxylase (*18*). A second subclass requires a pteridine ring as a cosubstrate, kinetically well studied examples being tyrosine hydroxylase (*19*) and phenylalanine hydroxylase (*20*). A third subclass that requires no cosubstrates for catalysis includes isopenicillin *N*-synthase that has been the subject of spectroscopic examination (*21*) and X-ray crystallography (*22*).

Since the discovery in 1979 that ACC is the direct precursor to ethylene formation (*4*), progress toward an ACC oxidase mechanism has been slow, due largely to the lack of purified enzyme and suitable in vitro assays. Thus, neither the kinetic nor catalytic mechanisms are well understood. Due to its important role in the regulation of plant development, a mechanistic understanding of ACC oxidase could provide a rational basis for its in vivo regulation. Furthermore, nonheme iron enzymes generally remain poorly

† This work was supported by the U.S. Department of Agriculture (NRICGP 93-37304-9161).

* To whom correspondence should be addressed. Phone: (805) 893-8368. Fax: (805) 893-4120. E-mail: reich@chem.ucsb.edu.

‡ Department of Chemistry and Biochemistry.

§ Department of Molecular, Cellular, and Developmental Biology.

[1] Abbreviations: AA, ascorbic acid or ascorbate; ACC, 1-aminocyclopropyl-1-carboxylic acid; AIB, α-aminoisobutyric acid; DHA, dehydroascorbic acid; D-Sac, D-saccharic 1,4-lactone; DTT, dithiothreitol; GC, gas chromatography; IPTG, isopropyl β-D-thiogalactopyranoside; MOPS, 3-(*N*-morpholino)propanesulfonic acid; TCA, trichloroacetic acid; Tris, tris(hydroxymethyl)aminomethane.

10.1021/bi0000162 CCC: $19.00
Published on Web 08/10/2000

Scheme 1: Reaction Stoichiometry of ACC Oxidase

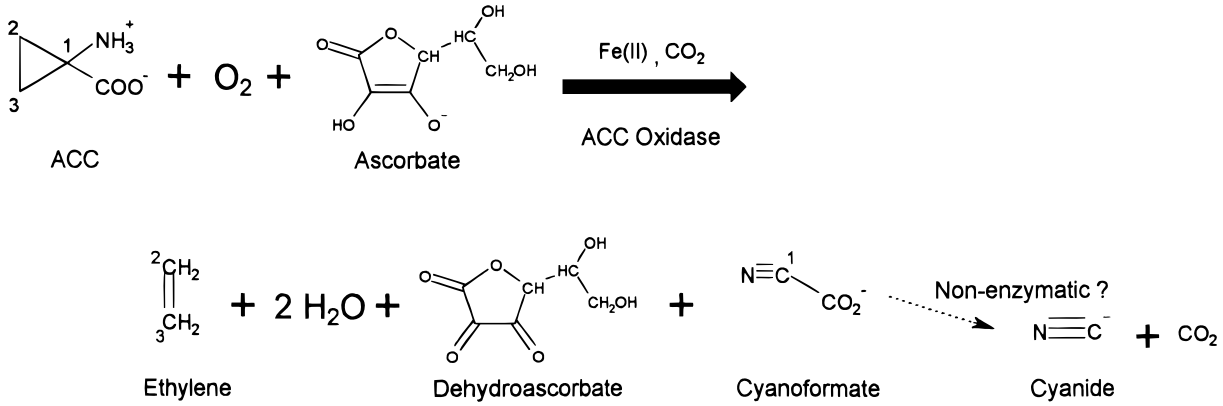

understood (*9*, *23*) despite their importance in both plant and animal metabolism. In this study, we used recombinant avocado ACC oxidase to develop a robust activity assay and assign the kinetic mechanism.

EXPERIMENTAL PROCEDURES

Materials. BSA (fraction V, 98% pure) was from ICN Biochemicals. Clorox brand bleach was used for 5% bleach solutions. $FeCl_2$, glycerol, TCA, certified ACS grade NaOH, trace metal grade HCl, EDTA, IPTG, DTT, and other standard buffers, media, and salts were from Fisher Scientific. Superoxide dismutase (3000 units/mg) and catalase (6609 units/mg) were from Calbiochem. Horseradish peroxidase (200 units/mg) and all other reagents were from Sigma.

Enzyme Expression System. A pET-3c expression plasmid containing the avocado ACC oxidase gene (*8*, *24*) was transformed into strain BL21(DE3) pLysS of *Escherichia coli* (Rolf E. Christoffersen et al., unpublished). Transformed *E. coli* were grown overnight at 37 °C in Luria−Bertani media with 50 μg/mL chloramphenicol and 200 μg/mL ampicillin. Overnight cultures were diluted 1:100 into 10 L of fresh media with the same composition and grown in an automated fermentor at 37 °C and with an O_2 concentration maintained at >100 μM to an OD_{550} of 0.15, at which time an additional 200 μg/mL ampicillin was added. Cultures were grown to an OD_{550} of 0.5 and then cooled to 27 °C. IPTG was added to 200 μM to induce expression for 5 h. Cells were harvested by centrifugation and resuspended in $^1/_{20}$th volume of buffer A [20 mM bis(2-hydroxyethyl)iminotris-(hydroxymethyl)aminomethane hydrochloride, pH 6.0, 0.1 mM Na_2EDTA, 1 mM DTT, 10% (v/v) glycerol] and then frozen slowly in order to aid lysis of the *E. coli* before overnight storage at −70 °C.

Purification of Overexpressed ACC Oxidase. All purification procedures were carried out at 4 °C, and all buffers were treated with Chelex 100 resin to remove divalent cations. After the cells were thawed slowly on ice, the paste was sonicated three times for 20 s each and then centrifuged at 20000*g* for 30 min. The supernatant was loaded directly onto a 5 × 35 cm Fast Flow Q Sepharose (Pharmacia) column equilibrated with buffer A plus 50 mM NaCl. The column was washed with 1 column volume of this buffer, and protein was eluted with a 0.5 L linear 50−500 mM NaCl gradient. The active fractions were pooled and concentrated under nitrogen in an Amicon ultrafiltration cell with YM10 membrane (Amicon Corp.). An equal volume of buffer B [50 mM Tris·HCl, pH 7.5, 0.1 mM Na_2EDTA, 1 mM DTT, 10% (v/v) glycerol] plus 3 M $(NH_4)_2SO_4$ was slowly added, and the mixture was immediately filtered through a Gelman Acrodisc 0.2 μm filter. This was then loaded onto a Pharmacia HR 10/10 alkyl-Superose column equilibrated with buffer B with 1.5 M $(NH_4)_2SO_4$. The column was run at 0.5 mL/min for 2 column volumes, and then the protein was eluted with a linear 120 mL gradient to 0 M salt. Active fractions were pooled, aliquoted, concentrated by ultrafiltration, and then passed through a G-25 Sephadex column equilibrated in buffer A without EDTA or DTT. The sample was immediately loaded onto a HR 10/10 Mono Q anion-exchange column (Pharmacia) equilibrated in the same buffer. The column was washed with 2 column volumes of buffer, and then protein was eluted with a linear 200 mL gradient of buffer A containing 500 mM NaCl, without EDTA or DTT. This step was necessary to purify the intact protein away from its major breakdown product. Purified ACC oxidase was frozen in liquid nitrogen and then stored at −70 °C.

General Enzyme Activity Assay. Unless otherwise noted, the standard assay was performed by filling 15 × 85 mm glass test tubes with 100 mM Na^+MOPS, pH 7.4, 2 mg/mL BSA, 12.5 mM AA, 20.0 μM $FeCl_2$·HCl, and 1.0 mM ACC to a volume of 300 μL. These substrate concentrations were considered optimal for maximum activity in our system. The tubes were then capped with Vacutainer rubber stoppers creating a 10 mL headspace over the liquid phase. An atmosphere of 5% CO_2 was created by adding 0.5 mL of CO_2 gas to ensure maximal activation (see below). Stock enzyme was placed on ice to thaw and then freshly diluted with cold dilution buffer (Chelexed 20 mM Na^+MOPS, pH 7.4, 70 mM NaCl, and 10% glycerol) to the desired concentration just prior to injection. No more than 20 μL of enzyme was used to initiate the reaction. Gastight syringes were used to deliver enzyme to the assay system and were equipped with Teflon plungers and Hamilton-type removable needles with Teflon gaskets to minimize the amount of metal contact during delivery.

Tubes were immediately placed in a vigorously (∼180 oscillations/min) shaking, 25 °C water bath for the desired amount of reaction time. The reaction was terminated by the injection of TCA to 7%, followed by 10 min of shaking to allow equilibration of ethylene between the liquid and gas phases. Evolved ethylene was measured by removing 3 mL of the headspace by syringe and injecting the sample onto a

GC (Hach Carle, series 400 AGC) outfitted with a 1/4 in. i.d. × 3 ft long stainless steel column packed with Poropack N 80/100 (Waters). Ethylene was separated on this column using helium as the carrier gas at a temperature of 70 °C and detected by a flame ionization detector (FID). A personal computer with Hewlett-Packard's 3365 Series II ChemStation software was used to collect the data from the GC and quantitate the area under the ethylene peak. The instrument was calibrated daily using standard ethylene (10 μL/L ± 5%, Scott Specialty Gases) as an external reference. The standard assay system presented here does not produce ethylene nonenzymatically (GC detection limit ≥1 nL/L), even after the addition of TCA, a strong acid. Additionally, the amount of TCA added is sufficient to terminate all enzymic activity.

All assay reagents were dissolved in NanoPure water (Barnstead) which had undergone Chelex treatment to reduce the introduction of adventitious transition state metals which severely inhibit the enzyme (*8*). Chelex treatment implies adding 1 mL/L of suspended Chelex-100 beads (Sigma) into solution and gently stirring overnight. If reagents were stored in glass containers, the Chelex beads were kept in solution to continuously bind metals leeching from the vessel's walls into the purified solutions (*25*). Preferably, clear plasticware was used to make up and store solutions since this material does not have significant contaminating metals (*26*). MOPS was chosen as a buffer in part because it does not chelate transition state metals (*27*). The SigmaUltra grade of buffer, titrated with trace metal-free grades of HCl and NaOH, was used exclusively to minimize the amount of introduced transition state metals. For the same reason, the sodium salt form of ascorbate was avoided, and instead the ACS reagent grade of ascorbic acid was used (*25*). Finally, all experiments were performed using certified metal-free pipet tips (Fisher Scientific).

For experiments requiring subatmospheric levels of O_2, the assay tubes were filled with buffer and BSA only, capped, and then flushed with 99.99% pure N_2 gas. The desired amount of oxygen was added by syringe. The tubes were shaken for 10 min to equilibrate the new atmosphere into the liquid phase. The reactions were terminated with 7% TCA that had been bubbled with pure N_2 gas for 15 min to avoid introducing any postreaction oxygen. After ethylene sampling, O_2 was determined by removal of 3 mL of headspace and injection onto a Shimadzu 6AM model GC equipped with a glass column (3 mm i.d. × 1.7 m long) packed with molecular sieve 5A 45/60 (Supelco). O_2 was separated using ultrapure helium as the carrier gas at 37 °C and 40 mL/min and detected by a thermal conductivity detector (TCD). The data were collected, and the area under the peak was quantitated with the HP ChemStation program, calibrated using ambient air (21% O_2) as an external standard. Absolute amounts of oxygen were measured in percent units, and these values were corrected to account for O_2 dilution incurred during the sampling process. Corrected percent units were then converted into μM O_2 dissolved in the liquid phase by assuming that 21% O_2 is equivalent to 240 μM dissolved oxygen and that a reduction in dissolved oxygen is linear with decreasing O_2 in the atmosphere.

Units of microliters per liter were converted into nanomoles of ethylene using the ideal gas law. The dilution by air that occurs during sampling was also taken into account. Reaction rates are always expressed in terms of specific activity using the standard unit of activity, that is, v = units/(mg·protein) = (μmol of product formed)/(min·mg of protein).

Substrate Calibration. The presence of redox active substrates is a serious cause for concern due to degradation in the substrate stocks themselves. For example, Fe(II) oxidizes in the presence of O_2 to form Fe(III), which forms a yellow precipitate in water, thus depleting the amount of available ferrous iron (*28*). AA is rapidly oxidized under neutral conditions into dehydroascorbate and water by just trace amounts of transition state metals, such as Fe(III) and Cu(II). Therefore, $FeCl_2$ stocks were prepared in 0.9 mM HCl to minimize oxidation to Fe(III) (*25*, *29*), and the free acid form of AA was used to create an acidic environment that greatly retards AA oxidation (*25*, *30*). Consequently, the acidity of the added reagents caused the initial pH of the assay buffer to drop 0.4 pH unit, although no further change was observed. Therefore, activity reported using an initial buffer pH of 7.4 describes a final assay pH of 7.0 at which the enzyme is reacting.

Calibrated substrate solutions were used to ensure accurate concentrations. AA solutions were freshly prepared, and then a small aliquot was diluted into 100 mM Na^+MOPS buffer, pH = 7.4. The absorbance at 265 nm was measured against a buffer blank, and the concentration of AA was calculated from Beer's law using an extinction coefficient of 14.5 mM^{-1} cm^{-1} (*25*). ACC was calibrated by its complete conversion into ethylene, accomplished nonenzymatically in 1 mL with $HgCl_2$ and a 2:1 mixture of bleach and 10 M NaOH (*31*). The evolved ethylene was quantitated by GC calibrated with an external standard. Fe(II) was calibrated by measuring the absorbance of iron−ferrozine complexes as described by Stookey (*32*).

AA is a very efficient ligand of Fe(II) at neutral pH, and the differentiation of Fe(II) into free and complexed species must be taken into account. The amount of free Fe(II) will change depending on the concentration of the AA ligand, and this may be calculated by eq 1, where K represents the equilibrium constant for complex formation and is equal to 1.62 under our experimental conditions (*33*). All Fe(II) values reported in this work are for the free species.

$$[\text{Fe(II)}]\text{total} = [\text{Fe(II)}]\text{free} + ([\text{Fe(II)}]\text{free}\cdot[\text{AA}]\text{free})/K \quad (1)$$

Data Analysis. Kinetic data were fit to the appropriate rate equations by the weighted least-squares method, assuming equal variances on the velocity parameters (*34*). The fitting programs of Cleland (*34*) were modified to run on a personal computer. Rectangular hyperbola curves obtained in the Michaelis constant determinations were fit to eq 2; substrates demonstrating substrate inhibition in the Michaelis constant determinations were fit to eq 3.

$$v = V_{max}A/[K_a + A] \quad (2)$$

$$v = V_{max}A/[K_a + A + (A_2/K_i)] \quad (3)$$

Reciprocal initial velocities were plotted against the reciprocal of the variable substrate concentration. Intersecting initial velocity patterns were fit to eq 4; parallel initial velocity patterns were fit to eq 5; initial velocity patterns which intersected on the *y*-axis when substrate A was the

Table 1: Purification of Avocado ACC Oxidase Overexpressed in *E. coli*

purification stage	specific activity [nmol min^{-1} (mg of protein)$^{-1}$]	fractional yield of oxidase activity	purification (*x*-fold)
crude extract	9.9	1	1
Fast Q Sepharose	39	0.86	3.9
alkyl-Superose	54	0.41	5.5
Mono Q	56	0.21	5.6

fixed variable substrate were fit to eq 6; and parallel initial velocity patterns which displayed double competitive substrate inhibition were fit to eq 7. When an inhibitor was varied against one of the substrates, the data were fit to either a linear competitive (eq 8), noncompetitive (eq 9), or uncompetitive (eq 10) rate equation.

$$v = V_{max}AB/[K_aB + K_bA + AB + K_{ia}K_b] \quad (4)$$

$$v = V_{max}AB/[K_aB + K_bA + AB] \quad (5)$$

$$v = V_{max}AB/[K_bA + AB + K_{ia}K_b] \quad (6)$$

$$v = V_{max}AB/[K_aB(1 + B/K_{ib}) + K_bA(1 + A/K_{ia}) + AB] \quad (7)$$

$$v = V_{max}A/[K_a(1 + I/K_{is}) + A] \quad (8)$$

$$v = V_{max}A/[K_a(1 + I/K_{is}) + A(1 + I/K_{ii})] \quad (9)$$

$$v = V_{max}A/[K_a + A(1 + I/K_{ii})] \quad (10)$$

A, *B*, and *I* refer to the concentration of substrates A and B and inhibitor, respectively. K_a and K_b are the Michaelis constants for those substrates; K_{ia} and K_{ib} are the dissociation constants. K_{is} and K_{ii} are inhibition constants with respect to the inhibitor's effect on the slope or intercept of the velocity.

RESULTS

Overexpression and Purification of Recombinant Avocado ACC Oxidase. Overexpressed ACC oxidase was purified 6-fold with a 21% yield (Table 1) and was estimated to be over 90% pure by Coomassie staining. Induction was performed at 27 °C rather than 37 °C to avoid having the majority of induced polypeptide occurring in an insoluble and inactive form (*35*). Furthermore, in crude extracts the overexpressed enzyme was slowly inactivated at 0 °C and required 100 μM Na_2EDTA for stability (Rolf E. Christoffersen et al., unpublished), possibly reflecting the sensitivity of ACC oxidase to various divalent cations (*8*, *36*). Thus EDTA was included in solutions throughout the purification, until the very last steps.

Various exogenous proteins were included in the reaction in an effort to further enhance the stability of ACC oxidase. Catalase, peroxidase, and superoxide dismutase were tested on the basis of their ability to remove damaging oxygen species that may be generated during enzymatic turnover. BSA was also included since it has been shown to stabilize a related nonheme iron enzyme (*37*). Identical assays were prepared with 100 mM Na^+MOPS, pH = 7.0, 4.5 mM AA, 1.35 mM $FeCl_2$, 0.1 mM ACC, 5% CO_2 gas, and 10 μg of enzyme and allowed to react for 10 min at 30 °C. Each data point in Figure 1 represents an average of three experiments.

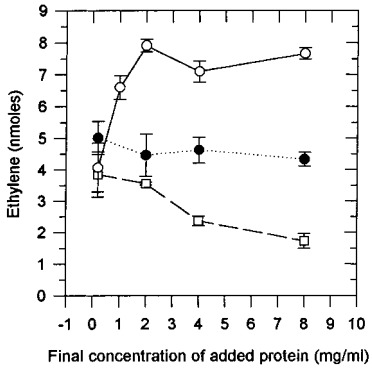

FIGURE 1: Effect of exogenous proteins on ACC oxidase activity: (○) bovine serum albumin; (●) horseradish peroxidase; (□) superoxide dismutase. Each data point reflects an average of three experiments.

Increasing concentrations of BSA enhanced activity in a linear fashion up to a maximum at 2 mg/mL, where activity was twice as high as without any added BSA [similar to previous results (*35*, *38*)]. Horseradish peroxidase displayed an initial 10−20% enhancement in activity at low levels of addition (0.1 mg/mL), beyond which no further effect was observed. Catalase exhibited behavior very similar to horseradish peroxidase (data not shown for clarity), which is in contrast to the substantial positive effect found by Smith et al. (*38*). Superoxide dismutase reduced the amount of activity with increasing levels of added protein. At the highest level of protein used (8 mg/mL), the activity had fallen by 50%.

Activity vs Time and Protein Concentration. ACC oxidase activity was measured as a function of time and protein concentration to verify that product formation was linear (100 mM Na^+MOPS, pH = 7.0, 2 mg/mL BSA, 4.5 mM AA, 13.5 μM $FeCl_2$, 0.1 mM ACC, and 5% CO_2 gas, at 25 °C). Ethylene values reported in Figure 2 are an average of two experiments.

ACC oxidase activity was linear up to about 30 min but then experienced a regular decrease with time. Consequently, our assays were run for no more than 30 min to ensure complete linearity (Figure 2A). No lag was observed within the first 2 min after enzyme addition (data not shown), indicating that the enzyme is quickly activated by CO_2 gas. Beyond 30 min, the reaction began to slow and eventually stopped. Complete conversion of the limiting substrate (ACC) could be achieved with 16 μg of enzyme (specific activity of 16 nmol min^{-1} mg^{-1}). Figure 2B shows that the number of turnovers in each assay is approximately the same and linear up 30 min.

Michaelis Constant Determinations. Reaction rates were measured under initial velocity conditions while varying a single substrate in order to determine the kinetic constants of all four components of the ACC oxidase reaction [Fe(II) was treated as a pseudosubstrate]. Figure 3 illustrates the results of the experiments when Fe(II) or ACC was varied. Normal Michaelis−Menten kinetics were obeyed initially; however, a progressive amount of activity was lost at higher substrate concentrations. These data sets were best fit by eq 3, which describes a reaction curve with substrate inhibition. Oxygen displayed normal Michaelis−Menten kinetics up to 350 μM (30% v/v), after which a dramatic loss in activity

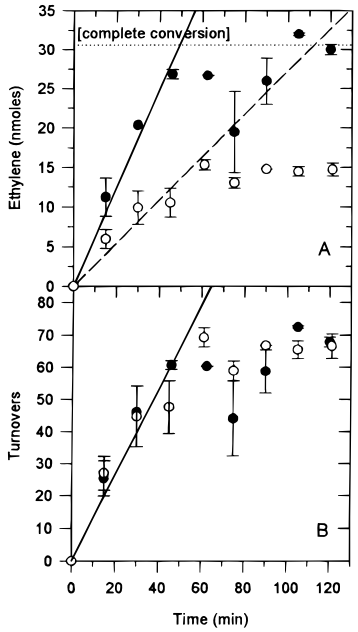

FIGURE 2: (A) Formation of product vs time as a function of ACC oxidase concentration. Protein amounts are (●) 16 μg and (○) 8 μg. The lines drawn are least-squares fits to the data from 0 to 45 min. (B) Enzyme turnover vs time comparison. Raw data are from panel A, and the line drawn is a least-squares fit to the data from 0 to 45 min. Values in both panels are from an average of two experiments.

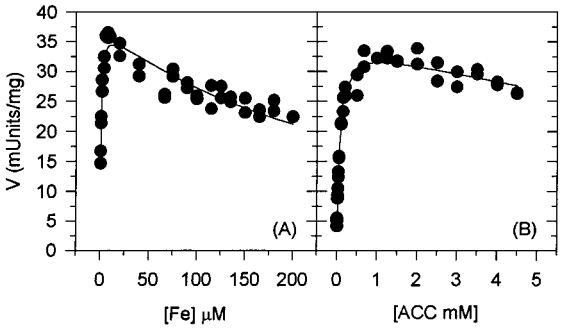

FIGURE 3: Michaelis constant determinations showing substrate inhibition. Assay conditions are as described in Experimental Procedures. Panels: (A) Fe(II); (B) ACC. Lines are drawn from the fit to eq 2.

Table 2: Substrate Michaelis Constants

constant	Fe(II)	AA	ACC	O_2
V_{max}[a]	38 ± 1	37 ± 1	35 ± 1	31 ± 1
K_m	40 ± 5 nM	2.1 ± 0.2 mM	62 ± 4 μM	4.4 ± 0.9 μM
K_{ia}	14.5 ± 1.38 μM		16.8 ± 2.9 mM	
K_{opt}[b]	2.3 μM	12.5 mM	1.0 mM	240 μM

[a] Milliunits per milligram. [b] K_{opt} is defined as the substrate concentration where the highest activity was observed under standard assay conditions and where all other substrates were at optimal concentrations.

was observed which is most likely due to nonenzymatic oxidation and inactivation (data not shown). The O_2 data followed a simple rectangular hyperbola and thus were best fit by eq 2. The kinetic constants obtained from these fits are listed in Table 2.

The reaction displayed a progressive loss of activity at high AA substrate concentrations that resembles substrate inhibition. This phenomenon, however, is in reality a manifestation of Fe−AA complex formation (see below).

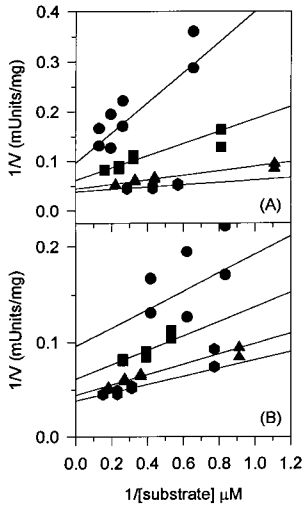

FIGURE 4: Double reciprocal plots demonstrating that Fe(II) and AA are bound to the enzyme as free entities. Assays were performed as described in Experimental Procedures using Fe(II) as the variable substrate and AA as the fixed variable substrate. Lines are drawn from a linear fit. AA concentrations: (●) = 0.5 mM; (■) = 1.0 mM; (▲) = 2.0 mM; (⬢) = 3.0 mM. Panels: (A) velocity vs the concentration of free Fe(II), which is a function of AA present; (B) velocity vs the concentration of the Fe−AA complex.

When the loss of activity due to complex formation is factored out, all "substrate inhibition" disappeared, and the data best fit a normal rectangular hyperbola as described by eq 2.

Since the Fe−AA complex is a significant species in solution, the possibility arises that the enzyme favors its binding over the free species. Steady-state kinetics can be used to determine whether the complex or free species are bound in the active site using the theory of Park et al. (*39*). Figure 4 displays double reciprocal plots of velocity vs either free Fe(II) or the Fe−AA complex. In both cases each fixed concentration of AA generated a separate reaction rate, indicating that the free species are the true substrates for the enzyme (*39*). Had all the data fallen on a single line, the complex would have been the true substrate.

Initial Velocity Studies. Table 3 summarizes the combinations of varied and nonvaried substrates studied and the kinetic constants obtained from data fits. An intersecting pattern is observed when Fe(II) and ACC were varied, with both AA and O_2 at optimal concentrations. A similar experiment at a lower concentration of AA (0.67 mM) did not change the intersecting pattern of lines. When Fe(II) and ACC were varied in the presence of low concentrations of both AA and O_2 (0.67 mM and 30 μM, respectively), the pattern did change and was best described by an equilibrium-ordered equation, with Fe(II) in thermodynamic equilibrium with the enzyme. This is further supported by our observation that when Fe(II) was varied with AA, the data best fit eq 6, suggesting that these two substrates bind in an equilibrium-ordered fashion and Fe(II) in thermodynamic equilibrium with the enzyme.

Oxygen was used as a variable substrate with each of the other substrates of the reaction. When oxygen was varied with either AA or ACC, the patterns could be fit well to the equilibrium-ordered equation, suggesting that O_2 was in thermodynamic equilibrium with the enzyme. When O_2 was varied with Fe(II), the pattern could be fit well to the

Table 3: Initial Velocity Experiments

varied substrates[a]	pattern[b]	V_{max} (milliunits/mg)	apparent K_a	apparent K_b
Fe vs AA (opt ACC, opt O_2)	EQORD	38 ± 2		1.3 ± 0.2 μM
Fe vs ACC (opt AA, opt O_2)	SEQ	38 ± 1	0.15 ± 0.01 μM	44 ± 5 μM
Fe vs ACC (low AA, opt O_2)	SEQ	10 ± 0.4	1.5 ± 0.2 μM	19 ± 2 μM
Fe vs ACC (low AA, low O_2)	EQORD	4.5 ± 0.4		58 ± 12 μM
Fe vs O_2 (opt ACC, opt AA)	EQORD	160 ± 190		140 ± 110 μM
Fe vs O_2 (low ACC, low AA)	SEQ	10 ± 1	79 ± 13 μM	1.2 ± 0.2 μM
AA vs ACC (opt Fe, opt O_2)	PPDCSIN	32 ± 1	1.2 ± 0.2 mM	26 ± 6 μM
AA vs ACC (opt Fe, low O_2)	SEQ	47 ± 16	49 ± 19 mM	0.42 ± 0.25 mM
AA vs O_2 (opt Fe, opt ACC)	EQORD	11 ± 2	86 ± 59 mM	
ACC vs O_2 (opt Fe, opt AA)	EQORD	22 ± 2	−6 ± 7 μM	

[a] Optimal concentrations of substrates: Fe = 2.3 μM, AA = 12.5 mM, ACC = 1.0 mM, and O_2 = 240 μM. Low concentrations: AA = 0.67 mM, ACC = 0.1 mM, and O_2 = 30 μM. [b] Abbreviations for patterns: EQORDO = equilibrium ordered (eq 6), SEQ = sequential (eq 4), and PPDCSIN = ping-pong with double competitive substrate inhibition (eq 7).

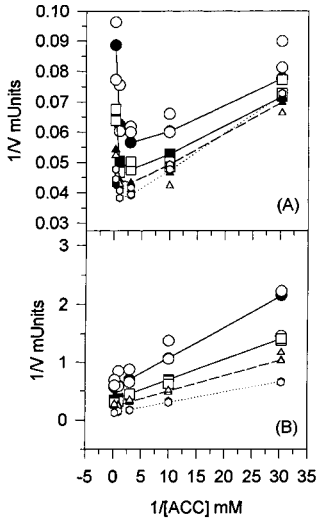

FIGURE 5: Initial velocity pattern observed when ACC is the variable substrate and AA is the fixed variable substrate using assay conditions as described in Experimental Procedures. Closed symbols represent data points from the calculated fit. Open symbols are experimental data. AA concentrations: (●, ○) = 2.0 mM; (■, □) = 3.3 mM; (▲, △) = 5.0 mM; (⬢, ⬡) = 10.0 mM. Panels: (A) assay under air-saturated conditions ([O_2] = 240 μM); (B) assay under reduced oxygen conditions ([O_2] = 30 μM).

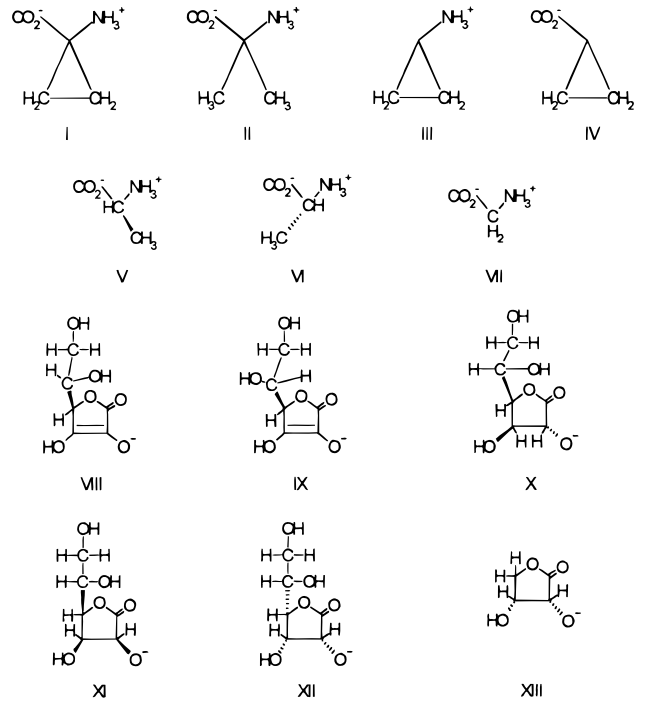

FIGURE 6: Inhibitors used in this study. ACC analogues: I = ACC, II = α-AIB, III = cyclopropylamine, IV = cyclopropane carboxylate, V = L-alanine, VI = D-alanine, and VII = glycine. AA analogues: VIII = AA, IX = isoascorbate, X = D-saccharic 1,4-lactone, XI = L-gulonic 1,4-lactone, XII = D-gulonic 1,4-lactone, and XIII = D-erythronic 1,4-lactone.

equilibrium-ordered equation. This experiment was repeated in the presence of low ACC and AA concentrations (0.10 mM and 0.67 mM, respectively), and the pattern changed to a sequential one.

The experiment in which AA and ACC were varied in the presence of optimal concentrations of the nonvaried substrates resulted in an atypical pattern, as shown in Figure 5A. While complex, this pattern is diagnostic for a system where parallel lines are complicated by competitive substrate inhibition from both varied substrates (*40*). This situation can be adequately described by eq 7, and the kinetic constants were obtained (Table 3). A dramatic change in the pattern of lines was observed when the oxygen concentration was lowered to suboptimal levels (30 μM). Figure 5B shows how, under otherwise identical conditions, the pattern transformed from a double competitive parallel pattern into a simple intersecting one, fitting well to eq 4.

Inhibition studies. A family of potential inhibitors (Figure 6) were chosen on the basis of their similarities to ACC, AA, or Fe(II), and their K_i constants were determined with respect to that substrate (Table 4). All AA analogues displayed competitive inhibition, and the best inhibitor was D-Sac. Isoascorbate behaved as a substrate for the reaction, so its kinetic constants were determined instead. It showed a higher K_m than AA (4.0 ± 0.8 mM) but also a higher maximum velocity (62 ± 7 milliunits/mg), so that the V/K values for isoascorbate and AA were the same (15 ± 1). All ACC analogues showed competitive inhibition except cyclopropylamine, which lacks a carboxyl group and showed uncompetitive inhibition vs ACC (K_i = 81 ± 12 mM). The best competitive inhibitor vs ACC was AIB. The dissociation constants of the ACC inhibitors were expressed in kilocalories per mole in order to gauge the relative binding energy contributions of each moiety in the ACC molecule. All Fe(II) inhibitors were competitive except for Cu(II), which displayed stronger than expected inhibition (data not shown). Metal−AA complexes were not considered an issue in these experiments since supersaturating concentrations of AA were not used.

Table 4: Inhibition Experiments

inhibitor	varied substrate[a]	pattern[b]	K_{is} (mM)	K_{ii} (mM)	binding energy (kcal/mol)
D-Sac	vs AA	C	0.41 ± 0.03		4.62
L-gulonic 1,4-lactone	vs AA	C	5.8 ± 0.5		3.05
D-gulonic 1,4-lactone	vs AA	C	73 ± 8		1.55
D-erythronic 1,4-lactone	vs AA	C	63 ± 10		1.64
AIB	vs ACC	C	2.0 ± 0.1		3.68
D-alanine	vs ACC	C	5.0 ± 0.2		3.14
L-alanine	vs ACC	C	24 ± 2		2.21
glycine	vs ACC	C	107 ± 21		1.32
cyclopropane carboxylic acid	vs ACC	C	7.6 ± 0.6		2.92
cyclopropylamine	vs ACC	UC		81 ± 12	
AIB	vs AA	C	18 ± 2		
AIB (low O_2)	vs AA	C	56 ± 7		
AIB	vs Fe	NC	60 ± 13	43 ± 16	
AIB	vs O_2	NI			
D-Sac	vs ACC	UC		1.4 ± 0.1	
D-Sac (low O_2)	vs ACC	NC	1.7 ± 0.2	5.7 ± 1.4	
D-Sac	vs Fe	C	0.21 ± 0.02		
D-Sac	vs O_2	UC		0.62 ± 0.04	
Co(II)	vs Fe	C	0.44 ± 0.04		
Zn(II)	vs Fe	C	0.59 ± 0.06		
Mn(II)	vs Fe	C	50 ± 4		

[a] All fixed substrates are at optimal concentrations: Fe = 2.3 μM, AA = 12.5 mM, ACC = 1.0 mM, and O_2 = 240 μM. Low O_2 = 30 μM. [b] Abbreviations for patterns: C = competitive (eq 8), NC = noncompetitive (eq 9), and UC = uncompetitive (eq 10). NI = no inhibition.

AIB and D-Sac were chosen for further kinetic analysis to confirm aspects of the kinetic mechanism; these data are included in Table 4. AIB was competitive with respect to AA, noncompetitive vs Fe(II), and showed no inhibition when O_2 was the variable substrate. The experiment with AA was repeated in the presence of low amounts of oxygen and the type of inhibition remained competitive, but the K_{is} was three times higher (see Table 3). D-Sac was a competitive inhibitor vs Fe(II) but uncompetitive vs O_2 and ACC.

DISCUSSION

An ACC oxidase assay is by necessity complex due to the number of substrates involved, the interference of nonenzymatic processes when they are mixed, the inherent instability of the purified protein, its activation by gaseous carbon dioxide, and the need to sample ethylene, another gaseous product. We have addressed each of these challenges in the development of our assay so that meaningful kinetic data could be drawn from it. Nevertheless, a decrease in enzymatic activity over longer time periods was observed and could not be explained by the complete consumption of a limiting substrate (Figure 2), revealing the limitations of our assay.

By working with the linear portion of the activity curve, a number of interesting results were observed that ran contrary to the published literature. Previously reported K_m-AA values of 10 and 16.7 mM (*41* and *35*, respectively) are much higher than the value of 2.1 mM measured here, most likely a consequence of previous work neglecting to account for nonenzymatic AA loss. ACC oxidase from banana and melon showed AA substrate inhibition (*8*, *36*, *41*), but these reports did not consider Fe−AA complex formation. We have used Park's methods (*39*) to show that the observed substrate inhibition is likely an artifact. When we plotted the AA K_m determination with calculated free AA concentrations, the curve changed to normal Michaelis−Menten kinetics.

Scheme 2: Proposed Kinetic Mechanism of ACC Oxidase[a]

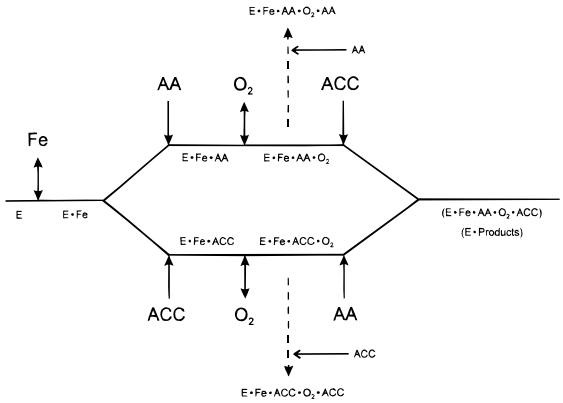

[a] Double-headed arrows denote a substrate in thermodynamic equilibrium with that enzyme form. Dashed arrows represent paths to dead-end complexes. Abbreviation: Fe = Fe(II).

The K_d for Fe(II) in avocado ACC oxidase is 40 nM and falls well below the values reported for other ACC oxidases which fall within a range of 1 and 19 μM (*35*, *41*, *42*). Maximum activity could be achieved with as little as 0.8 μM Fe(II), which is approximately the amount of enzyme present in the assay, implying a stoichiometric occupation of Fe(II) into all available active sites. Higher levels of Fe(II) began to inhibit the enzyme, which might be due to a second, allosteric metal binding site which weakly binds Fe(II) and causes the substrate inhibition seen in Figure 3B. The presence of a second site was invoked to explain some ACC oxidase protein fragmentation results (*43*); however, the existence of a second site has not yet been definitely proven and must remain highly speculative. ACC oxidase's substrate inhibition with respect to Fe(II) is shared by giberellin C-20 hydroxylase (*44*) and prolyl hydroxylase (*45*).

Kinetic Mechanism. A kinetic mechanism for ACC oxidase that models all of the data in Table 3 is presented in Scheme 2. Our proposal is somewhat different than those suggested for related nonheme enzymes since we suggest the enzyme

can bind either AA or ACC after O_2 addition (Table 3), implying a random mechanism. The observation of substrate inhibition in a number of key steps lends credence to our proposal.

The double competitive substrate inhibition observed with AA and ACC and optimal O_2 concentrations (Figure 5A) is consistent with a second molecule of the first substrate binding to the enzyme after oxygen, instead of the expected second substrate. The position of substrate inhibition is placed after O_2 binding since lowering the O_2 concentration removed the inhibition (Figure 5B). ACC oxidase is more susceptible to substrate inhibition by AA than ACC, since the K_i/K_m ratios are 16 and 62, respectively, yet is the preferred route for substrate binding indicated by the lower thermodynamic binding constant ($K_{ia}O_2$) value with AA. Notably, the two forms of substrate inhibition occur only after oxygen has bound, implying that the active site becomes receptive to binding various substrates after binding oxygen. The placement of Fe(II) binding before the random element of the model was determined by varying Fe(II) and AA or ACC, where the patterns observed were equilibrium ordered and sequential, respectively.

The kinetic mechanism for ACC oxidase presented here is based solely on initial velocity kinetics and must be considered a working model until confirming experiments are conducted using different techniques. Nevertheless, our proposed kinetic mechanism for ACC oxidase is similar in some respects to those presented for other mononuclear nonheme iron enzymes, such as tyrosine hydroxylase (*19*) which exhibits an ordered addition of Fe(II) and pterin cosubstrate, followed by the equilibrium-ordered addition of O_2, and ending with the addition of tyrosine. Tyrosine hydroxylase also displays well-characterized substrate inhibition, where tyrosine competes competitively with the enzyme form with which the pterin cosubstrate should bind, implicating a second tyrosine binding in the pterin binding pocket. An analogous situation is likely for ACC oxidase.

ACC oxidase may tolerate a random mechanism since none of its substrates undergoes permanent oxygen atom incorporation, unlike the nonheme iron pterin- or α-ketoglutarate-dependent enzymes. In the latter cases, molecular oxygen is split and the first atom is incorporated into the cosubstrate (*17*); thus the cosubstrate binds and is oxidized first to generate a reactive Fe−O species, which in turn oxidizes the second substrate by atomic oxygen incorporation. This is not the case in ACC oxidase chemistry, and its random mechanism may in fact provide a clue to how it catalyzes its reaction.

Substrate Binding Topology. Our study of various substrate analogues identified structural requirements of the substrates that are critical for binding. The results in Table 4 show that the most important elements for ACC binding in descending order are the carboxyl, C_3, the amino group, and C_2. The carboxylate may be of prime importance because it directly coordinates to the nonheme iron (*46*). The poor inhibition seen with D-alanine may be tied to the fact that the only alternate substrate ACC oxidase will tolerate is an ethyl or methyl substituent on the C_2 carbon of ACC (*47*). The C_3 carbon atom was clearly more important with regard to binding, since its absence (L-alanine) causes a serious loss in inhibition. C_2 and C_3 each contribute independent amounts of binding energy because the energy loss from each carbon is additive, as borne out by the binding energy of glycine which lacks either.

With regard to AA binding, ACC oxidase exhibits a distinct preference for the position of the hydroxyl groups attached to these carbons to be trans in contrast to the planar lactone ring of AA, its natural substrate. This is borne out by D-Sac, which displayed the most potent inhibition and is identical to AA except that its C_2-C_3 bond is fully saturated and the attending hydroxyls are in the trans position. If the C_2 hydroxyl is moved into the cis position (L-gulonic lactone), the inhibitor strength drops, while moving the C_3 hydroxyl into the cis position (D-gulonic lactone), the loss of inhibition strength becomes even more severe. ACC oxidase does not significantly interact with the side chain of AA. Isoascorbate differs only in the stereochemistry of the hydroxyl group around C_5, the first carbon atom in the side chain, yet is accepted by the enzyme as a good substrate with a V/K value equal to AA. In addition, the K_i constant for erythronic lactone is approximately the same as that for D-gulonic lactone despite the complete lack of a side chain (see Figure 6). The importance of the side chain of AA has been investigated previously for prolyl hydroxylase and was also found not to be critical to substrate binding (*48*). In contrast, research with the tomato enzyme (*35*) ascribed an important role to the side chain since the ascorbate analogues D-ascorbate and 5,6-*O*-isopropylidine L-ascorbate were substrates whereas L-galactono-γ-lactone was completely inactive.

In conclusion, we anticipate that these studies will be a foundation for further enzymological and crystallographic studies to build upon. With the crystal structures of the free enzyme and the enzyme bound to the substrate analogues identified here, aspects of the proposed kinetic mechanism and substrate binding determinants will be affirmed or refined. The unique chemistry which ACC oxidase catalyzes is likely to differentiate it from related nonheme enzymes.

REFERENCES

1. Reid, M. S. (1987) in *Plant Hormones and Their Role in Plant Growth and Development* (Davies, P. J., Ed.) pp 257−279, Martinus Nijhoff Publishers, Dordrecht, The Netherlands.
2. McKeon, T. A., Fernandez-Maculet, J. C., and Yang, S.-F. (1995) in *Plant Hormones* (Davies, P. J., Ed.) 2nd ed., pp 118−139, Kluwer Academic Publishers, Amsterdam, The Netherlands.
3. Stella, L., Wouters, S., and Baldellon, F. (1996) *Bull. Soc. Chim. Fr. 133*, 441−455.
4. Adams, D. O., and Yang, S. F. (1979) *Proc. Natl. Acad. Sci. U.S.A. 76*, 170−174.
5. Ververidis, P., and John, P. (1991) *Phytochemistry 30*, 725−727.
6. Fernández-Maculet, J. C., and Yang, S. F. (1992) *Plant Physiol. 99*, 751−754.
7. Kuai, J., and Dilley, D. R. (1992) *Postharvest Biol. Technol. 1*, 203−211.
8. McGarvey, D. J., and Christoffersen, R. E. (1992) *J. Biol. Chem. 267*, 5964−5967.
9. Feig, A. L., and Lippard, S. J. (1994) *Chem. Rev. 94*, 759−805.
10. Dong, J. G., Frenández-Maculet, J. C., and Yang, S. F. (1992) *Proc. Natl. Acad. Sci. U.S.A. 89*, 9789−9793.
11. Peiser, G. D., Wang, T.-T., Hoffman, N. E., Yang, S. F., Liu, H.-W., and Walsh, C. T. (1984) *Proc. Natl. Acad. Sci. U.S.A. 81*, 3059−3063.
12. Adams, D. O., and Yang, S. F. (1981) *Trends Biochem. Sci. 6*, 161−164.

13. Poneleit, L. S., and Dilley, D. R. (1993) *Postharvest Biol. Technol. 3*, 191−199.
14. Fernández-Maculet, J. C., Dong, J. G., and Yang, S. F. (1993) *Biochem. Biophys. Res. Commun. 193*, 1168−1173.
15. Myllylä, R., Tuderman, L., and Kivirikko, K. I. (1977) *Eur. J. Biochem. 80*, 349−357.
16. Puistola, U., Turpeenniemi-Hujanen, T. M., Myllylä, R., and Kivirikko, K. I. (1980) *Biochim. Biophys. Acta 611*, 40−50.
17. Blanchard, J. S., and Englard, S. (1983) *Biochemistry 22*, 5922−5929.
18. Holme, E. (1975) *Biochemistry 14*, 4999−5003.
19. Fitzpatrick, P. F. (1991) *Biochemistry 30*, 3658−3662.
20. Benkovic, S. J., Bloom, L. M., Bollag, G., Dix, T. A., Gaffney, B. J., and Pember S. (1986) *Ann. N.Y. Acad. Sci. 471*, 226−232.
21. Baldwin, J. E., and Bradley, M. (1990) *Chem. Rev. 90*, 1079−1088.
22. Roach, P. L., Clifton, I. J., Fülöp, V., Harlos, K., Barton, G. J., Hajdu, J., Andersson, I., Schofield, C. J., and Baldwin, J. E. (1995) *Nature 375*, 700−704.
23. Prescott, A. G. (1993) *J. Exp. Biol. 44*, 849−861.
24. McGarvey, D. J., Yu, H., and Christoffersen, R. E. (1990) *Plant Mol. Biol. 15*, 165−167.
25. Buettner, G. R. (1988) *J. Biochem. Biophys. Methods 16*, 27−40.
26. Fish, W. W. (1988) *Methods Enzymol. 158*, 357−364.
27. Good, N. E., and Izawa, S. (1972) *Methods Enzymol. 24*, 53−68.
28. Sienko, M. J., and Plane, R. A. (1966) in *Chemistry: Principles and Properties*, McGraw-Hill, New York.
29. Dorey, C., Copper, C., Dickson, D. P. E., Gibson, J. F., Simpson, R. J., and Peters, T. J. (1993) *Br. J. Nutr. 70*, 157−169.
30. Sauberlich, H. E., Green, M. D., and Omaye, S. T. (1982) in *Ascorbic Acid: Chemistry, Metabolism, and Uses* (Seib, P. A., and Tolbert, B. M., Eds.) Vol. 200, pp 199−221, Advances in Chemistry Series, American Chemical Society, Washington, DC.
31. Lizada, M. C. C., and Yang, S. F. (1979) *Anal. Biochem. 100*, 140−145.
32. Stookey, L. L. (1970) *Anal. Chem. 42*, 779−781.
33. Martell, A. E., and Smith, R. M. (1977) *Critical Stability Constants*, Vol. 3, Plenum Publishing Corp., New York.
34. Cleland, W. W. (1979) *Methods Enzymol. 63*, 103−138.
35. Zhang, Z., Schofield, C. J., Baldwin, J. E., Thomas, P., and John, P. (1995) *Biochem. J. 307*, 77−85.
36. Smith, J. J., Ververidis, P., and John, P. (1992) *Phytochemistry 31*, 1485−1494.
37. Blanchard, J. S., Englard, S., and Kondo, A. (1982) *Arch. Biochem. Biophys. 219*, 327−334.
38. Smith, J. J., Zhang, Z. H., Schofield, C. J., John, P., and Baldwin, J. E. (1994) *J. Exp. Bot. 45*, 521−527.
39. Park, S.-H., Kiick, D. M., Harris, B. G., and Cook, P. F. (1984) *Biochemistry 23*, 5446−5453.
40. Cleland W. W. (1979) *Methods Enzymol. 63*, 500−513.
41. Moya-Leon, M. A., and John, P. (1995) *Phytochemistry 39*, 15−20.
42. Pirrung, M. C., Kaiser, L. M., and Chen, J. (1993) *Biochemistry 32*, 7445−7450.
43. Barlow, J. N., Zhang, Z., John, P., Baldwin, J. E., and Schofield, C. J. (1997) *Biochemistry 36*, 3563−3569.
44. Lange, T., and Graebe, J. E. (1989) *Planta 179*, 211−221.
45. Tuderman, L., Myllylä, R., and Kivirikko, K. I. (1977) *Eur. J. Biochem. 80*, 341−348.
46. Rocklin, A. M., Tierney, D. L., Kofman, V., Brunhuber, N. M. W., Hoffman, B. M., Christoffersen, R. E., Reich, N. O., Lipscomb, J. D., and Que, L., Jr. (1999) *Proc. Natl. Acad. Sci. U.S.A. 96*, 7905−7909.
47. Hoffman, N. E., Yang, S. F., Ichihara, A., and Sakamura, S. (1982) *Plant Physiol. 70*, 195−199.
48. Tschank, G., Sanders, J., Baringhaus, K.-H., Dallacker, F., Kivirikko, K. I., and Günzler, V. (1994) *Biochem. J. 300*, 75−79.

BI0000162